A Systematic Study on Activation Processes in Organotellurium-Mediated Living Radical Polymerizations of Styrene, Methyl Methacrylate, Methyl Acrylate, and Vinyl Acetate

Yungwan Kwak,[†] Atsushi Goto,[†] Takeshi Fukuda,*[,†] Yu Kobayashi,[‡] and Shigeru Yamago*[,‡,§]

Institute for Chemical Research, Kyoto University, Uji, Kyoto 611-0011, Japan, and Division of Molecular Material Science, Graduate School of Science, Osaka City University, and PREST, Japan Science and Technology Corporation, Osaka 558-8585, Japan

Received February 8, 2006; Revised Manuscript Received April 13, 2006

ABSTRACT: The activation processes for the organotellurium-mediated living radical polymerizations (TERPs) of styrene (St), methyl methacrylate (MMA), methyl acrylate (MA), and vinyl acetate (VAc) were systematically studied. For the St, MMA, and MA homopolymerizations, both thermal dissociation and degenerative chain transfer (DT) were involved in the activation process with the main mechanism being DT at the examined temperatures (40−100 °C). The degenerative (exchange) chain transfer constant C_{ex} increased in the order of MMA < St ∼ MA. The temperature dependence of C_{ex} was weak and negative for these monomers. The VAc homopolymerization also included DT as the main activation mechanism. For the VAc polymerization, head-to-head monomer addition is significant on propagation, forming a primary alkyl chain-end (−CH_2−$TeCH_3$) adduct. The activation of this adduct was too slow to yield low-polydispersity polymers, explaining why the polydispersity control is not satisfactory for VAc at high degrees of polymerization. The C_{ex} for a poly(methyl methacrylate) (PMMA) radical to PMMA−$TeCH_3$ (homopolymerization) and polystyrene−$TeCH_3$ (block copolymerization) adducts were similar, suggesting that the DT in TERP is a (nearly) single-step reaction without forming a kinetically important intermediate.

Introduction

Living radical polymerization (LRP) has attracted much attention in the past decade as a robust and versatile method for preparing well-defined, low-polydispersity polymers.[1−6] The basic concept of LRP is reversible activation−deactivation processes (Scheme 1a). The dormant species P−X is activated by thermal, photochemical, and/or chemical stimuli to produce the propagating radical P•. In the presence of monomer M, P• will undergo propagation until it is deactivated back to P−X. A number of activation−deactivation cycles allow all the chains to have an almost equal chance of growing, yielding low-polydispersity polymers. Thus, sufficiently large k_{act} and k_{deact} are a requisite to obtain low-polydispersity polymers in a reasonable period of time; k_{act} and k_{deact} are the generalized (pseudo-first-order) rate constants of activation and deactivation, respectively (Scheme 1a).

Yamago et al. developed organotellurium-mediated LRP (TERP) as a novel class of LRP.[6−11] TERP exhibits good polydispersity controllability for a variety of monomers, including styrenics, acrylates, and methacrylates, suggesting sufficiently large k_{act} values for these monomers. It can also provide copolymers with well-defined structures and is tolerant of functional groups. TERP is thus a powerful synthetic tool to access novel functional materials.

We previously studied the activation process for the TERP of styrene (St) at 60 and 100 °C.[11] Both thermal dissociation (TD: Scheme 1b) and degenerative (exchange) chain transfer (DT: Scheme 1c) were involved in the activation process with the main mechanism being DT. When the polymerization proceeds solely by DT mechanism, the rates of activation and deactivation naturally equal to that of exchange reaction (cf. eq 1). Therefore, we concluded that the observed high level of control in the styrene polymerization is mainly due to the large k_{ex} value at this range of temperature. In this work, we systematically studied the activation processes for St, methyl methacrylate (MMA), methyl acrylate (MA), and vinyl acetate (VAc) at various temperatures to establish the activation mechanisms and obtain the Arrhenius parameters of the relevant rate constants. We also studied the activation process for the block copolymerizations of St and MMA to obtain more detailed information about the DT process for TERP.

Scheme 1. Reversible Activation Processes in Living Radical Polymerization (X = −TeMe in This Work)

(a) Reversible Activation

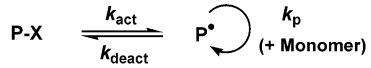

(X = -TeMe in This Work)

(b) Thermal Dissociation (TD)

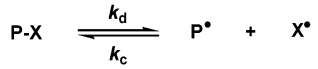

(c) Degenerative (Exchange) Chain Transfer (DT)

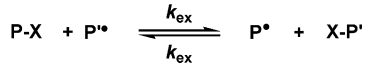

[†] Kyoto University.
[‡] Osaka City University and PREST, Japan Science and Technology Corporation.
[§] Current address: Institute for Chemical Research, Kyoto University, Uji, Kyoto 611-0011, Japan.
* Corresponding authors. E-mail: fukuda@scl.kyoto-u.ac.jp; yamago@scl.kyoto-u.ac.jp.

10.1021/ma060295m CCC: $33.50
Published on Web 06/08/2006

Definition. TERP possibly includes TD and DT as the activation mechanisms. If both processes coexist, k_{act} will take the form

$$k_{act} = k_d + k_{ex}[P^\bullet] \quad (1)$$

in which k_d and k_{ex} are the rate constants for TD and DT, respectively (Scheme 1). Thus, by determining k_{act} as a function of the polymerization rate R_p (hence $[P^\bullet]$), we can obtain k_d and k_{ex}.

Experimental Section

Materials. St (99%, Nacalai Tesque, Japan), MMA (99%, Nacalai), MA (99%, Nacalai), VAc (99%, Nacalai), azobis(isobutyronitrile) (AIBN; 98%, Wako Pure Chemical, Japan), and 2,2′-azobis(2,4,4-trimethylpentane) (VR110; 99.9%, Wako) were purified by distillation or recrystallization. Ethyl 2-methyltellanyl-2-methylpropionate (EMA-TeMe) was prepared as previously described.[8]

Measurements. The gel permeation chromatography (GPC) analysis was made on a Shodex GPC-101 liquid chromatograph (Tokyo, Japan) equipped with two Shodex KF-804L polystyrene (PSt) mixed gel columns (300 × 8.0 mm; bead size = 7 μm; pore size = 20−200 Å). Tetrahydrofuran (THF) was used as eluent with a flow rate of 0.8 mL/min (40 °C). Sample detection and quantification were made with a Shodex differential refractometer RI-101 calibrated with known concentrations of polymers in THF. The column system was calibrated with standard PSts and poly(methyl methacrylate)s (PMMAs). The number- and weight-average molecular weights M_n and M_w, respectively, for poly(methyl acrylate) (PMA) and poly(vinyl acetate) (PVAc) were determined by the universal calibration method[12] using the Mark−Houwink−Sakurada constants, $K = 0.0114$ mL/g and $a = 0.716$ for PSt,[13] $K = 0.0195$ mL/g and $a = 0.660$ for PMA,[13] and $K = 0.0156$ mL/g and $a = 0.708$ for PVAc,[14] where K and a are defined as $[\eta] = KM^a$, with $[\eta]$ and M being the intrinsic viscosity and molecular weight, respectively. For two PVAc samples (see below), sample detection was also made with a multiangle laser light scattering (MALLS) detector, a Wyatt Technology DAWN EOS (Santa Barbara, CA), equipped with a Ga−As laser (λ = 690 nm). The refractive index increment dn/dc was determined to be 0.0430 mL g^{-1} by a Wyatt Technology OPTILAB DSP differential refractometer.

Preparative GPC was performed on a Japan Analytical Industry LC-928R machine (Tokyo) equipped with JAIGEL 1H and 2H PSt gel columns (600 × 20 mm; bead size = 16 μm; pore size = 20−30 (1H) and 40−50 (2H) Å) using chloroform as eluant.

IR spectra were recorded on a Shimadzu FTIR-8200PC spectrometer (Kyoto) and are reported in cm^{-1}.

HRMS spectra were obtained on a JEOL (Japan Electron Optics Laboratory, Tokyo) AX500 spectrometer under EI (electron impact) ionization conditions with applied voltage of 70 keV.

^{1}H and ^{13}C NMR spectra were recorded on a JEOL JNM-AL400 (400 MHz) at ambient temperature with flip angle 45°. ^{1}H: spectral width 7936.5 Hz, acquisition time 4.129 s, and pulse delay 10.0 s. ^{13}C: 27027.0 Hz, 1.212 s, and 1.784 s.

Preparation of Polymer−Methyltellurides. The synthesis, purification, and storage of polymer−methyltellurides were made under a nitrogen or an argon atmosphere. A solution of St with EMA−TeMe (230 mM) was heated at 100 °C for 9 h.[7] After purification by reprecipitation from methanol, a PSt−TeMe with $M_n = 3000$ and $M_w/M_n = 1.17$ was isolated. The chain extension test[15] showed that this polymer contained 3% ($f_{dead} = 0.03$) of potentially inactive species without a TeMe moiety at the chain end, for which the experimental data shown below have been corrected. PMMA−TeMe ($M_n = 2500$, $M_w/M_n = 1.07$, $f_{dead} = 0.03$) and PMA−TeMe ($M_n = 3000$, $M_w/M_n = 1.10$, $f_{dead} = 0.05$) were similarly prepared.[8] PVAc−TeMe adducts ($M_n = 3100$, $M_w/M_n = 1.28$, $f_{dead} < 0.05$ and $M_n = 7000$, $M_w/M_n = 1.50$, $f_{dead} < 0.1$) were prepared by heating a VAc solution of EMA−TeMe (100 mM) and AIBN (100 mM) at 60 °C (for 1 and 2 h, respectively) and then by reprecipitation from cold diethyl ether. The f_{dead} for the PVAc−TeMe adducts could not be accurately determined by the chain extension test (due to the very slow activation of the primary alkyl chain-end adduct included in these polymers (see below)). Thus, the experimental data for them have not been corrected for f_{dead}. However, the relevant errors are within 10%, since f_{dead} was less than 0.1 for these polymers.

Preparation of 1-(Methyltellanyl)ethyl Acetate (VAc−TeMe). Methyllithium (25.5 mL, 0.98 M solution in diethyl ether, 25 mmol) was slowly added to a suspension of tellurium powder (2.93 g, 23 mmol) in 25 mL of THF over 20 min at 0 °C. The resulting mixture was stirred for 30 min at room temperature until tellurium powder disappeared. 1-Iodoethyl acetate (5.35 g, 25 mmol)[16] was added to this solution at 0 °C, and the resulting solution was stirred at room temperature for 1.5 h. Water was added to this solution, and the aqueous layer was separated using a cannula under a nitrogen atmosphere. The remaining organic phase was washed with saturated aqueous NH_4Cl solution and saturated aqueous NaCl solution, dried over $MgSO_4$, and filtered under a nitrogen atmosphere. Solvent was removed under reduced pressure followed by distillation under reduced pressure (21.5−27.0 °C/1.4−2.2 mmHg) to give a 86:14 mixture of the titled compound and dimethyl ditelluride (1.34 g: yield of the titled compound was 22%). The mixture was further purified by preparative GPC under a nitrogen atmosphere followed by vacuum distillation (58.5 °C/5.5 mmHg) to give a pure sample as yellow oil. IR (neat): 2926, 1734, 1369, 1234, 1055, 1015, 934, 845. HRMS (EI) m/z: Calcd for $C_5H_{10}O_2Te$ $(M)^+$, 231.9743; Found: 231.9725; ^{1}H NMR (400 MHz, $CDCl_3$): 1.85 (d, J = 6.8 Hz, 3H), 2.05 (s, 3H), 2.07 (s, 3H), 6.39 (q, J = 6.8 Hz, 1H). ^{13}C NMR (100 MHz, $CDCl_3$): 20.80 (CH_3), 21.45 (CH_3), 24.61 (CH_3), 49.22 (CH), 170.23 (C).

Determination of k_{act} for Polymer−Methyltellurides. The five polymer−methyltellurides described above were used as probe adducts (P_0−Xs). A mixture of monomer(s) (3 mL), a P_0−X (5.4 mM), and an azo-initiator (AIBN: 0−70 mM at 40−70 °C or VR110: 0−40 mM at 80−100 °C) in a Schlenk flask was heated at a prescribed temperature T under an argon atmosphere. After a prescribed time t, an aliquot (0.1 mL) of the solution was taken out by a syringe, quenched to room temperature, diluted by THF to a known concentration, and analyzed by GPC.

Determination of k_{ex} for VAc−TeMe. A mixture of VAc (1 mL), AIBN (5.0 mM), and VAc−TeMe (0−5.4 mM) in a Schlenk flask was heated at 60 °C for 15 min, diluted by THF, and analyzed by GPC. The k_{ex} was determined from the Mayo plot (see below) using the M_n obtained by the universal calibration method (UC) in the range of M_n = 1000−14 000. To confirm the validity of the UC-based M_n in this range, two PVAc samples (P_0−Xs (see above)) were analyzed by GPC-MALLS. The M_n values (3200 and 7100) obtained by GPC-MALLS well agreed with those (3100 and 7000, respectively) obtained by UC.

Results and Discussion

Homopolymerization of St. We previously reported the results for 60 and 100 °C polymerizations without giving experimental details and full discussion.[11] Here we give those for 60 °C, along with the results and discussion for 40−100 °C.

A solution of St including a fixed amount of PSt−TeMe (5.4 mM) as a probe P_0−X and variable amounts of AIBN (0−26 mM) as a conventional radical initiator was heated at 60 °C. Figure 1 shows examples of the GPC curves for t = 40 min. An increment of the area relative to that for $t = 0$ shows the amount of the monomer converted to polymer. Figure 2 shows the first-order plot of the monomer concentration [M]. The plot was linear in the examined range of time in all cases. From the slope of the line, we obtained $R_p/[M]$. Figure 3 shows the plot of $(R_p/[M])^2$ vs $[AIBN]_0$. The plot (filled circles) was linear, and the open circle for the conventional system (without PSt−

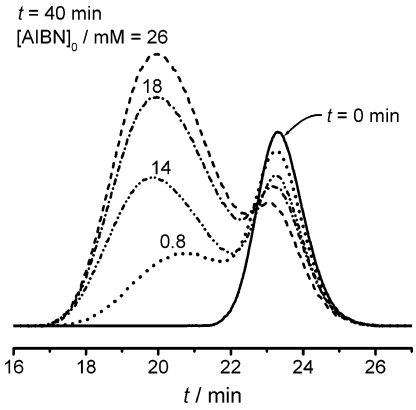

Figure 1. Examples of the gel permeation chromatography (GPC) charts for the styrene/polystyrene−TeMe (P_0−X)/azobis(isobutyronitrile) (AIBN) system (in bulk) (60 °C): $[P_0-X]_0 = 5.4$ mM; $[AIBN]_0$ as indicated in the figure.

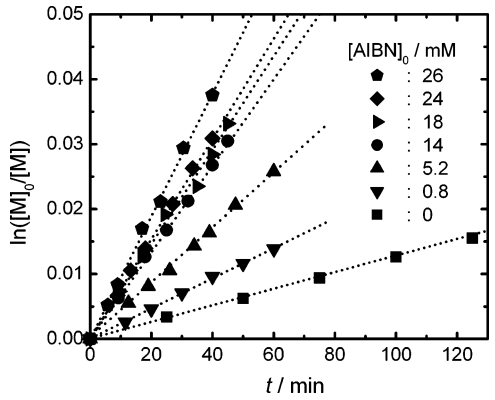

Figure 2. Plot of $\ln([M]_0/[M])$ vs t for the styrene (St)/polystyrene−TeMe (P_0−X)/azobis(isobutyronitrile) (AIBN) system (in bulk) (60 °C): $[P_0-X]_0 = 5.4$ mM; $[AIBN]_0$ as indicated in the figure. The [M] is the concentration of monomer (St).

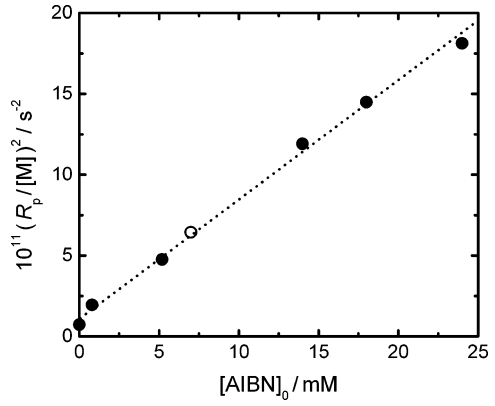

Figure 3. Plot of $(R_p/[M])^2$ vs $[AIBN]_0$ for the styrene (St)/polystyrene−TeMe (P_0−X)/azobis(isobutyronitrile) (AIBN) system (in bulk) (60 °C): $[P_0-X]_0 = 0$ (○) and 5.4 mM (●); $[AIBN]_0$ as indicated in the figure. The R_p is the polymerization rate, and [M] is the concentration of monomer (St).

TeMe) fell on the same line. This means that the organotellurium has no significant effect on R_p and that, as in the conventional system, R_p follows the conventional rate law

$$R_p = k_p(R_i/k_t)^{1/2}[M] \quad (2)$$

in which k_p is the propagation rate constant, k_t is the termination rate constant, and R_i is the conventional initiation rate. The R_i is the sum of the initiation rates due to the thermal initaition of

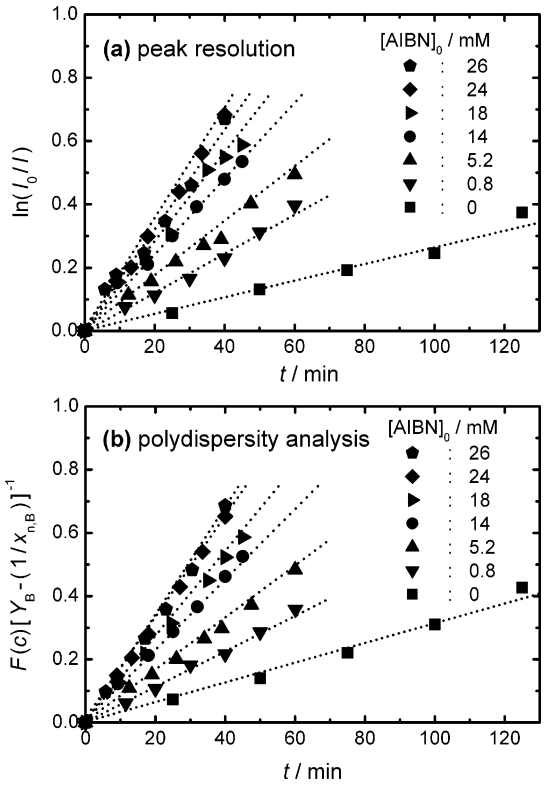

Figure 4. Plots of (a) $\ln(I_0/I)$ vs t and (b) $F(c)[Y_B - (1/x_{n,B})]^{-1}$ vs t for the styrene/polystyrene−TeMe (P_0−X)/azobis(isobutyronitrile) (AIBN) system (in bulk) (60 °C): $[P_0-X]_0 = 5.4$ mM; $[AIBN]_0$ as indicated in the figure. The I is [P_0−X], and $F(c)[Y_B - (1/x_{n,B})]^{-1}$ is defined in eq 4.

St and the decomposition of AIBN. Equation 2 held at all examined (40−100 °C) temperatures.

The k_{act} was determined by the GPC peak resolution method.[4,5,17] When P_0−X is activated to $P_0^\bullet$, the $P_0^\bullet$ will propagate until it is deactivated to give a new adduct P_1−X. (The subscripts 0 and 1 denote the numbers of activation.) Since P_0−X and P_1−X are generally different in chain length and its distribution, they may be distinguishable by GPC. By following [P_0−X], k_{act} can be determined from

$$\ln(I_0/I) = k_{act}t \quad (3)$$

in which I_0 and I are the concentrations of P_0−X at times zero and t, respectively. A lower $[P_0-X]_0$ leads to a larger number of monomer units added to $P_0^\bullet$ during an activation−deactivation cycle.[4,5,18] In fact, with a sufficiently low $[P_0-X]_0$ (5.4 mM in this case), GPC chromatograms (Figure 1) were composed of two peaks, allowing accurate resolution. The lower-molecular-weight component corresponds to P_0−X, and the higher-molecular-weight one corresponds to P_1−X and other minor species such as the further activated chains (P_2−X, etc.). Figure 4a shows the plot of $\ln(I_0/I)$ vs t for various [AIBN]. The plot was linear in all cases, from which we obtained k_{act}.

We alternatively determined k_{act} by the polydispersity analysis method.[4,5,19] We used the following relations that are valid for the "ideal" LRP in which reactions other than activation, deactivation, and propagation are absent, and [P•] is constant.

$$Y = w_A{}^2Y_A + w_B{}^2Y_B \quad (4)$$

$$F(c)[Y_B - (1/x_{n,B})]^{-1} = k_{act}t \quad (5)$$

Here the product polymer at time t is viewed as an A−B block

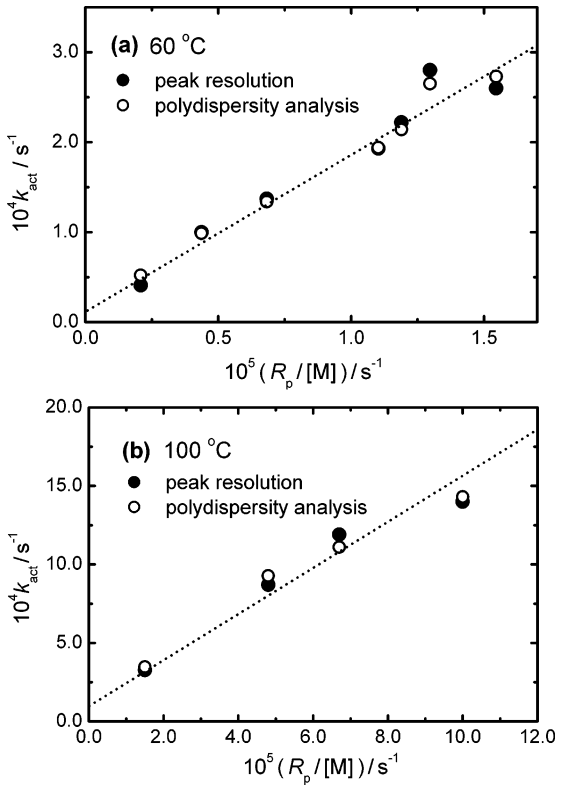

Figure 5. Plot of k_{act} vs (R_p/[M]) for the styrene (St)/polystyrene−TeMe system (in bulk) at (a) 60 and (b) 100 °C. The pseudo-first-order activation rate constant k_{act} (defined in Scheme 1a) was determined by the peak resolution method (●) and the polydispersity analysis method (○). The R_p is the polymerization rate, and [M] is the concentration of monomer (St).

copolymer with the subchains A and B referring to P_0−X and the incremental (grown) portion of the chain, respectively; $Y = (x_w/x_n) - 1$, $Y_K = (x_{w,K}/x_{n,K}) - 1$, $w_A = 1 - w_B = x_{n,A}/x_n$, $x_n = x_{n,A} + x_{n,B}$, and x_n and x_w are the number- and weight-average degrees of polymerization (K = A or B); the function $F(c)$ of the fractional conversion c is given by $F(c) = (1 - 2c^{-1}) \ln(1 - c)$ for a *batch* polymerization. We can measure the overall degrees of polymerization (x_n and x_w) and those of the subchain A ($x_{n,A}$ and $x_{w,A}$) by GPC. We can then calculate $x_{n,B}$ and Y_B according to eq 4 and determine k_{act} according to eq 5. Prerequisites for this method to be valid are the constancy of both [P•] and the number of polymer chains N_p. The concentration [N_p] estimated by c and x_n exceeded in no case 5% of [P_0−X]$_0$, which, along with the linear plot in Figure 2, confirms that the prerequisites were approximately met in this experiment.

Figure 4b shows the plot of $F(c)[Y_B - (1/x_{n,B})]^{-1}$ vs t, from which we obtained k_{act}.

Figure 5a shows the plot of k_{act} vs R_p/[M] (= k_p[P•]) at 60 °C according to eq 1. The peak resolution (filled circle) and polydispersity analysis (open circle) methods gave almost identical k_{act}. The plot was linear, and from the intercept and slope of the line (the best-fit line given by the least-squares methods), we obtained $k_d = 1 \times 10^{-5}$ s^{-1} and the exchange constant C_{ex} (= k_{ex}/k_p) = 17, respectively. Figure 5b shows the same plot at 100 °C, at which thermal dissociation was more clearly observed ($k_d = 1.5 \times 10^{-4}$ s^{-1}). The C_{ex} was 15 at 100 °C. (The previously reported C_{ex} value of 20 at 100 °C[11] was found to be inaccurate due to the contaminant in the employed probe polymer. It should be replaced by the value 15 in this report. The k_d value was virtually unchanged.) Thus, TERP involves two activation processes, of which DT (degenerative chain transfer) is the main one, as shown by these figures. (The error in the obtained C_{ex} is small (within 10% at 95% confidence level), and that in the k_d is large (within a factor of 2). Despite a large error, the best-fit line gave a nonzero positive k_d for the mentioned two systems (and all other St, MMA, and MA systems shown below), suggesting the dual activation mechanism.)

For a batch DT system, the smallest possible M_w/M_n (PDI) of the product is expected at full conversion (c = 1) and is given by eq 6, when the "initiating" moiety (A subchain) is neglected.[5,18]

$$x_w/x_n = 1 + C_{ex}^{-1} + x_n^{-1} \quad (c = 1) \tag{6}$$

With C_{ex} = 17 at 60 °C, this is calculated to be 1.06 at $x_n^{-1} \sim 0$, explaining why this system can afford low-polydispersity polymers ($M_w/M_n \sim 1.1$). (Strictly speaking, the theoretical PDI is somewhat smaller than 1.06 due to the small contribution of thermal dissociation.) The C_{ex} for X = methyltellanyl (17 at 60 °C) in this work was larger than that for X = iodide (4.0)[18] and smaller than those for X = dimethylstibanyl (33)[20] and dithioacetate (180)[21] (Table 1). This is consistent with the observed performance of the relevant DT polymerizations in terms of the polydispersity controllability.

Figure 6 shows the temperature dependence of k_{ex} at 40−100 °C, where k_{ex} was calculated with the obtained C_{ex} and the literature k_p[22] (C_{ex} = k_{ex}/k_p). The result is given by eq 7.

$$k_{ex}/(\mathrm{M}^{-1}\,\mathrm{s}^{-1}) = 2.8 \times 10^8 \exp(-30.0\ \mathrm{kJ\ mol}^{-1}/RT) \tag{7}$$

The activation energy E_{ex} of 30.0 kJ mol^{-1} is similar to that for X = iodide (27.8 kJ mol^{-1})[18] and larger than those for X =

Table 1. k_d, k_{ex}, k_p, C_{ex}, and the Arrhenius Parameters for k_{ex} for Homopolymerizations[a]

		k_{ex}					
P−X[b]	k_d (s^{-1}) (60 °C)	A_{ex} [c] (M^{-1} s^{-1})	E_{ex} [d] (kJ mol^{-1})	k_{ex} (M^{-1} s^{-1}) (60 °C)	k_p [e] (M^{-1} s^{-1}) (60 °C)	C_{ex} (60 °C)	ref for k_d, k_{ex}, and C_{ex}
PSt−TeMe	1×10^{-5}	2.8×10^8	30.0	5.8×10^3	3.4×10^2	17	this work
PMMA−TeMe	5×10^{-6}	4.0×10^6	20.0	3.0×10^3	8.3×10^2	3.6	this work
PMA−TeMe	$\leq 1 \times 10^{-3}$	4.9×10^5	0.0[f]	4.6×10^5	2.4×10^4	19	this work
PVAc−TeMe (secondary)[g]	~0			$1.0\ (\pm 0.3) \times 10^6$	9.5×10^3	110 ± 30	this work
PVAc−TeMe (primary)[h]	~0			1.1×10^4	9.5×10^3	1.2	this work
VAc−TeMe				2.8×10^5	9.5×10^3	30	this work
PSt−I	~0	3.1×10^7	27.8	1.4×10^3	3.4×10^2	4.0	18
PSt−$SbMe_2$	~0	3.9×10^7	22.6	1.1×10^4	3.4×10^2	33	20
PSt−SCSMe	~0	1.3×10^8	21.0	6.1×10^4	3.4×10^2	180	21

[a] The k_d, k_{ex}, and k_p are the rate constants of thermal dissociation (Scheme 1b), degenerative (exchange) chain transfer (Scheme 1c), and propagation, respectively, and C_{ex} is the exchange constant defined by $C_{ex} = k_{ex}/k_p$. [b] PSt, PMMA, PMA, and PVAc are polystyrene, poly(methyl methacrylate), poly(methyl acrylate), and poly(vinyl acetate), respectively, and VAc−TeMe is 1-(methyltellanyl)ethyl acetate. [c] Frequency factor of k_{ex}. [d] Activation energy of k_{ex}. [e] Literature value: refs 22, 23, 13, and 36 for styrene, methyl methacrylate, methyl acrylate, and vinyl acetate, respectively. [f] Apparent value (see the text). [g] The (ordinary) secondary alkyl chain end (−CH(OCOMe)−TeMe) adduct. [h] The (head-to-head) primary alkyl chain end (−CH_2−TeMe) adduct.

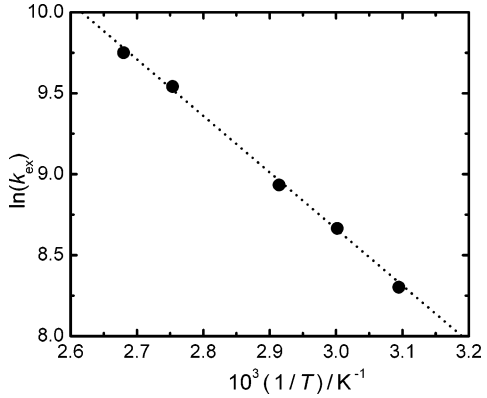

Figure 6. Plot of ln(k_{ex}) vs 1/T for the styrene/polystyrene−TeMe system (in bulk). The k_{ex} is the degenerative (exchange) chain transfer rate constant (defined in Scheme 1c), and T is temperature.

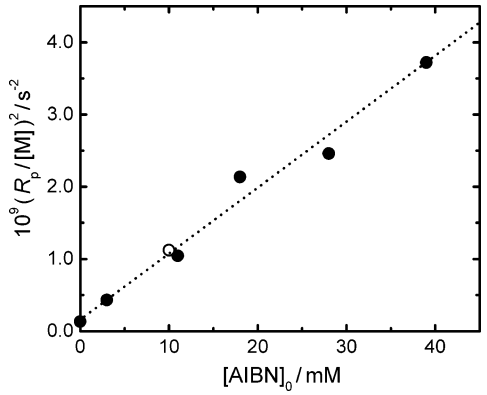

Figure 7. Plot of $(R_p/[M])^2$ vs $[AIBN]_0$ for the methyl methacrylate (MMA)/poly(methyl methacrylate)−TeMe (P_0−X)/azobis(isobutyronitrile) (AIBN) system (in bulk) (60 °C): $[P_0-X]_0 = 0$ (○) and 5.4 mM (●); $[AIBN]_0$ as indicated in the figure. The R_p is the polymerization rate, and [M] is the concentration of monomer (MMA).

dimethylstibanyl (22.6)[20] and dithioacetate (21.0)[21] (Table 1). The temperature dependence of C_{ex} is given by eq 8.

$$C_{ex} = 6.5 \exp(+2.5 \text{ kJ mol}^{-1}/RT) \quad (8)$$

The weak (negative) temperature dependence of C_{ex} suggests that temperature does not largely affect the polydispersity controllability.

Homopolymerization of MMA. The MMA polymerization was studied at 45−90 °C. The first-order plot of [M] was linear at all temperatures. Figure 7 shows the plot of $(R_p/[M])^2$ vs $[AIBN]_0$ at 60 °C with (filled circles) and without (open circle) PMMA−TeMe, showing the validity of eq 2. Equation 2 held at all studied temperatures. Parts a and b of Figure 8 show the plot of k_{act} vs R_p/[M] at 60 and 90 °C, respectively. Both TD and DT were involved in the activation process, and DT (degenerative chain transfer) was the main activation process, as in the St system. The C_{ex} was 3.6 and 3.2 at 60 and 90 °C, respectively. These C_{ex} values are too small to yield low-polydispersity polymers (M_w/M_n will exceed 1.28 at 60 °C and 1.31 at 90 °C according to eq 6). For the MMA polymerization, the addition of dimethyl ditelluride $(MeTe)_2$ was effective to yield low-polydispersity polymers ($M_w/M_n \sim 1.1$), while without its addition, M_w/M_n was larger than 1.35.[8,11] This means that k_{act} increases in the presence of $(MeTe)_2$. We are now examining this issue, which will be reported in a forthcoming paper.

Figure 9 shows the temperature dependence of k_{ex}, where k_{ex} was calculated with the obtained C_{ex} and the literature k_p.[23]

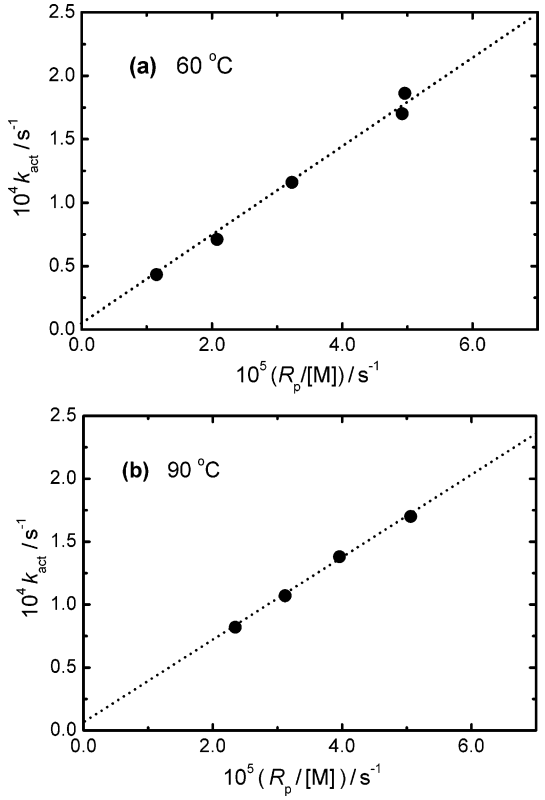

Figure 8. Plot of k_{act} vs $(R_p/[M])$ for the methyl methacrylate (MMA)/poly(methyl methacrylate)−TeMe system (in bulk) at (a) 60 and (b) 90 °C. The pseudo-first-order activation rate constant k_{act} (defined in Scheme 1a) was determined by the peak resolution method. The R_p is the polymerization rate, and [M] is the concentration of monomer (MMA).

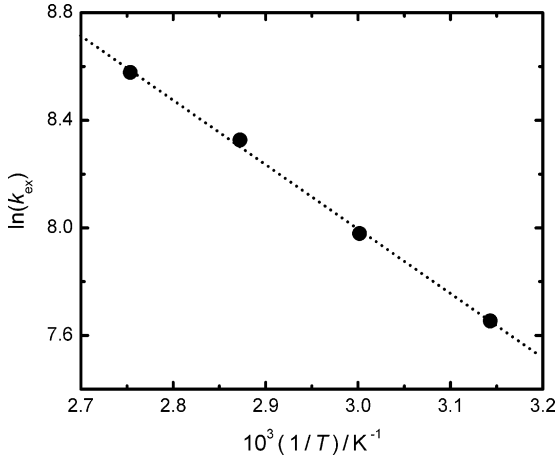

Figure 9. Plot of ln(k_{ex}) vs 1/T for the methyl methacrylate/poly(methyl methacrylate)−TeMe system (in bulk). The k_{ex} is the degenerative (exchange) chain transfer rate constant (defined in Scheme 1c), and T is temperature.

The temperature dependences of k_{ex} and C_{ex} were represented by eqs 9 and 10, respectively.

$$k_{ex}/(\text{M}^{-1}\text{ s}^{-1}) = 4.0 \times 10^6 \exp(-20.0 \text{ kJ mol}^{-1}/RT) \quad (9)$$

$$C_{ex} = 1.5 \exp(+2.3 \text{ kJ mol}^{-1}/RT) \quad (10)$$

The C_{ex} was weakly and negatively dependent on temperature, as in the St system.

Homopolymerization of MA. We examined the MA system at 40−70 °C. At all temperatures, R_p approximately followed

Scheme 2. Formation of Midchain Radical by Intramolecular Chain Transfer (Backbiting)

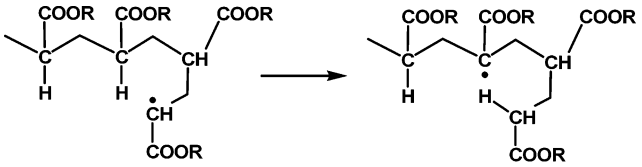

eq 2, as in the St and MMA systems. Parts a and b of Figure 10 show the plot of k_{act} vs R_p/[M] at 40 and 60 °C, respectively. The MA system also involved both TD and DT, and DT was the main process. The C_{ex} was 19 at 60 °C, which is similar to that for St (17) and larger than that for MMA (3.6). Therefore, C_{ex} largely depends on polymers (or monomers). The temperature dependences of k_{ex} and C_{ex} at 40−70 °C are given by

$$k_{ex}/(\mathrm{M}^{-1}\,\mathrm{s}^{-1}) = 4.9 \times 10^5 \exp(0.0\ \mathrm{kJ\ mol}^{-1}/RT) \quad (11)$$

$$C_{ex} = 0.14 \exp(+13.9\ \mathrm{kJ\ mol}^{-1}/RT) \quad (12)$$

in which k_{ex} was calculated with the literature k_p.[13] The observed (apparent) zero activation energy for k_{ex} would be explained as follows. For acrylate polymerizations, conventional intramolecular chain transfer (Scheme 2) (sometimes referred to as backbiting) is significant. This reaction produces the midchain radical, which is less reactive than the ordinary chain-end radical, and the fraction of the midchain radical increases with an increase in temperature.[24] (For *n*-butyl acrylate, for example, the fraction of the midchain radical increases from 70% at 30 °C to 85% at 60 °C.[25]) Thus, although the k_{ex} for both the chain-end and midchain radicals should increase with temperature, the increase in the fraction of the less reactive midchain radical may have canceled the increases in k_{ex}, leading to the apparent independence on temperature. (The overall k_{ex} can increase with temperature due to the increases in k_{ex} for the two radicals and can decrease due to the increase in the fraction of the less reactive radical. The increase and decrease may have been canceled in this case.)

PMA−TeMe can accordingly include the chain-end and midchain adducts formed from the corresponding radicals. For PMA−TeMe, the fractions of the two adducts could not be measured by ^{1}H NMR due to the overlap of the relevant signals. For poly(*n*-butyl acrylate)−TeMe, we could estimate the fraction of the chain-end adduct to be >95% by ^{1}H NMR (Supporting Information). This suggests that the P_0−X (PMA−TeMe) used in this work mainly consisted of the chain-end adduct and therefore that we may take the obtained k_{ex} and k_d as those for the chain-end adduct.

Homopolymerization of VAc. The TERP of VAc provides low-polydispersity polymers at low degrees of polymerization (DPs), but the controllability decreased at high DPs.[26] This was also noticed in the iodide-mediated LRP[16] and iron-catalyzed LRP[27] (atom transfer radical polymerization) of VAc. For the propagation of VAc, head-to-head (h−h) addition is known to be significant.[28] The h−h addition will give a primary alkyl chain-end radical (−$CH_2^{\bullet}$), which, followed by deactivation, will form a primary alkyl chain-end adduct. If the activation of the primary adduct is ineffective, low-polydispersity polymers are not achievable at high DPs, even if the activation of the (ordinary) secondary alkyl chain-end adduct is sufficiently fast. This explanation was proposed for the iodide and iron systems.[16,27]

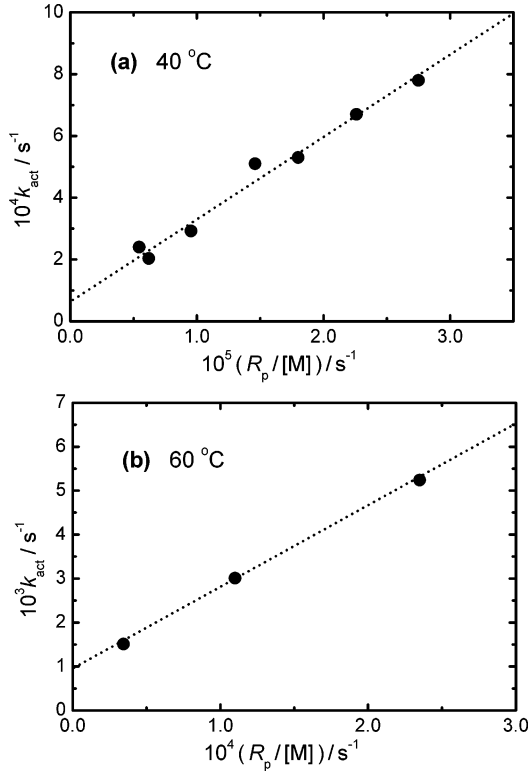

Figure 10. Plot of k_{act} vs (R_p/[M]) for the methyl acrylate (MA)/poly(methyl acrylate)−TeMe system (in bulk) at (a) 40 and (b) 60 °C. The pseudo-first-order activation rate constant k_{act} (defined in Scheme 1a) was determined by the peak resolution method. The R_p is the polymerization rate, and [M] is the concentration of monomer (MA).

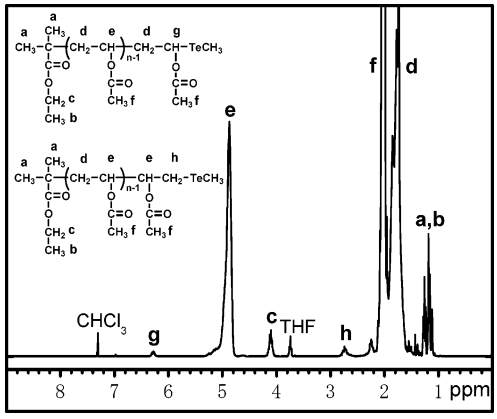

Figure 11. ^{1}H NMR spectrum of the poly(vinyl acetate)−TeMe with M_n = 3100 (x_n = 34) and M_w/M_n = 1.26. The synthetic condition for this polymer is given in the text.

To assess this in the TERP, we analyzed the chain-end structures of the polymers formed in the TERP by ^{1}H NMR. Figure 11 shows the spectrum of the polymer formed in the TERP of VAc (10 M) with EMA−TeMe (100 mM) and AIBN (100 mM) at 60 °C for 1 h, which had M_n = 3100 (x_n = 34) and M_w/M_n = 1.28 according to GPC. From the areas of the signals for the CH_2 protons (**c**) at the initiating moiety and the CH_3 protons at the monomer unit (**f**), we estimated x_n to be 36, which is close to the GPC value. (The amount of the AIBN-initiated chain was negligible (<5%) due to the short polymerization time, 1 h.) In Figure 11, the signal for the CH_2 protons (**h**) at the h−h primary chain end as well as that for the CH proton (**g**) at the ordinary secondary chain end clearly appeared. From the areas for these signals, we estimated the fraction (f_{sec}) of the ordinary secondary adduct to be 0.42 (42%). Similarly,

we analyzed the polymer with $x_n = 93$ and $M_w/M_n = 1.50$ formed for 2 h to obtain $f_{sec} = 0.10$. This confirms the significant formation of the primary adduct in the TERP.

We used the polymer with $f_{sec} = 0.10$ as a probe P_0-X to determine k_{act} by the peak resolution method at 60 °C. The $[P_0-X]$ rapidly decayed by about 10% within the conversion of 5% and slowly decayed thereafter. The former rapid decay corresponds mainly to the activation of the more reactive ordinary secondary adduct, and the latter slow decay corresponds to that of the less reactive primary adduct. From the latter decay, we estimated the k_{act} for the primary adduct. Figure 12a shows the plot of the k_{act} vs $R_p/[M]$. The plot was linear, from which we had $C_{ex} = 1.2$. This value is too small to give low-polydispersity polymers. Then, we used the polymer with $f_{sec} = 0.42$ as a P_0-X. We followed the initial fast decay and estimated the k_{act} for the secondary adduct (assuming no activation of the primary adduct). This was a rough estimate, since we followed a small decay of the GPC peak height (only 21% height decay at the 50% decay of the probe secondary adduct concentration). Figure 12b shows the plot of k_{act} vs $R_p/[M]$, yielding $C_{ex} = 110 \pm 30$. This value is large enough to give low-polydispersity polymers. The plot also suggested that $k_d \sim 0$. By the Mayo method,[29] we determined the C_{ex} for a low-mass secondary adduct, VAc−TeMe (Me−CH(OCOMe)−TeMe), which is a pure secondary adduct. We heated a solution of VAc (10 M) with a fixed amount of AIBN (5.0 mM) and variable amounts of VAc−TeMe (0−5.4 mM) at 60 °C for 10 min (conversion = ca. 0.5%) and determined the C_{ex} according to[29]

$$\frac{1}{x_n} = \frac{1}{x_{n,0}} + C_{ex}\left(\frac{I_0}{[M]_0}\right) \tag{13}$$

in which I_0 and $[M]_0$ are the concentrations of the adduct and monomer at $t = 0$, respectively, and x_n and $x_{n,0}$ are the number-average DPs of the produced polymers with and without the adduct, respectively. Figure 13 shows the Mayo plot. The plot was linear, from which we obtained $C_{ex} = 30$. This value is again large enough to yield low-polydispersity polymers. (The difference by a factor about 3.7 (= 110/30) between the C_{ex} values for the polymer and monomer analogues may be explained by the usual chain length dependence.[5]) Thus, the poor polydispersity controllability at high DPs is attributed to the formation of the primary adduct and its too slow activation.

When the primary adduct does not undergo activation, f_{sec} will decrease with x_n as

$$f_{sec} = (1 - p_{hh}p_{deact})^{x_n} \tag{14}$$

in which p_{hh} is the probability of h−h addition in propagation, p_{deact} is the probability for the thereby formed primary radical to undergo deactivation rather than propagation, and p_{hh} and p_{deact} are assumed to be independent of x_n. The p_{deact} is given by

$$p_{deact} = \frac{k_{ex}[P_{sec}-X]}{k_{ex}[P_{sec}-X] + k_p[M]} = \left(1 + \frac{[M]}{C_{ex}[P_{sec}-X]}\right)^{-1} \tag{15}$$

in which $P_{sec}-X$ is the secondary adduct. Note that k_{ex}, k_p, and hence C_{ex} in eq 15 are those specific to the primary radical.

For the preparation of the mentioned polymer with $x_n = 34$ and $f_{sec} = 0.42$, the activation of the formed primary adduct was negligible due to the small C_{ex} (and the relatively small conversion of 35%). The constancies of p_{hh} and p_{deact} were approximately valid, since p_{hh} and C_{ex} should not strongly depend on x_n (in the polymer range), and the ratio $[M]/[P_{sec}-X]$ did not significantly change (100 at $t = 0$ and 150 at $t = 1$ h). Thus, eq 14 may be applied to this system, from which we had $p_{hh}p_{deact} = 0.025$. Assuming that the C_{ex} for the primary radical is identical to that for the secondary radical, we obtained $p_{deact} = 0.52$ according to eq 15 with $[M]/[P_{sec}-X] = 100$ and $C_{ex} = 110$ (obtained in the actual polymerization with mainly the secondary radical (see above)). With this p_{deact} and $p_{hh}p_{deact} = 0.025$, we have $p_{hh} = 0.048$. This is comparable in magnitude with the literature value of 0.017.[28] The difference may be ascribed to the employed (possibly unsuitable) C_{ex}. In the limit

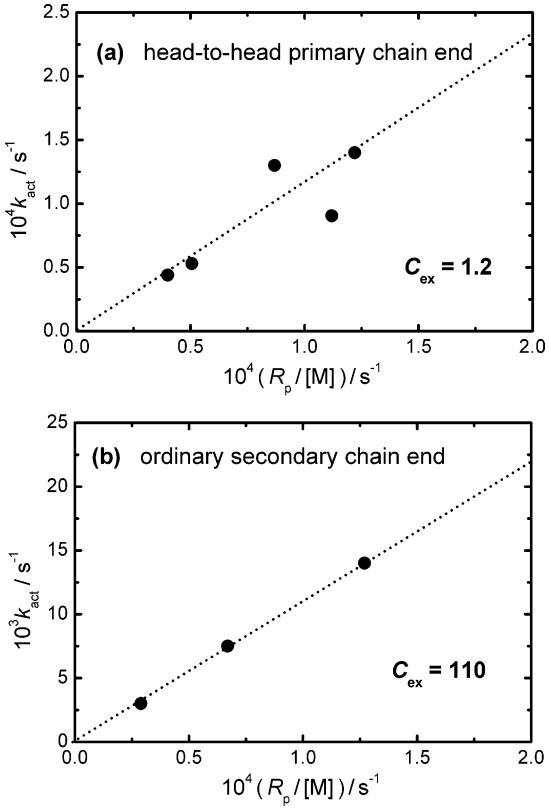

Figure 12. Plot of k_{act} vs $(R_p/[M])$ for the vinyl acetate (VAc)/poly(vinyl acetate)−TeMe systems (in bulk) (60 °C) for (a) (head-to-head) primary chain-end adduct and (b) (ordinary) secondary chain-end adduct. The pseudo-first-order activation rate constant k_{act} (defined in Scheme 1a) was determined by the peak resolution method. The R_p is the polymerization rate, and [M] is the concentration of monomer (VAc).

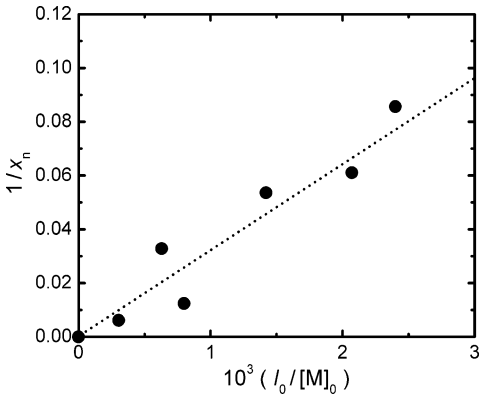

Figure 13. Mayo plot for the vinyl acetate (VAc)/1-(methyltellanyl)-ethyl acetate (VAc−TeMe)/azobis(isobutyronitrile) (AIBN) system (in bulk) (60 °C): $[VAc-TeMe]_0 = I_0 = 0-5.4$ mM; $[AIBN]_0 = 5.0$ mM. The x_n is the number-average degree of polymerization, and $[M]_0$ is the concentration of monomer (VAc) at time zero.

Table 2. C_{ex} for Homopolymerizations and Block Copolymerizations of St and MMA (60 °C)[a]

	PSt•	PMMA•
PSt−TeMe	17	2.8
PMMA−TeMe	31	3.6

[a] The C_{ex} is the exchange constant defined by $C_{ex} = k_{ex}/k_p$, where k_{ex}, and k_p are the rate constants of degenerative (exchange) chain transfer (Scheme 1c) and propagation, respectively. St, MMA, PSt, and PMMA are styrene, methyl methacrylate, polystyrene, and poly(methyl methacrylate), respectively.

Scheme 3. Energy Diagrams for (a) Single-Step and (b) Two-Step Degenerative Chain Transfer Reactions

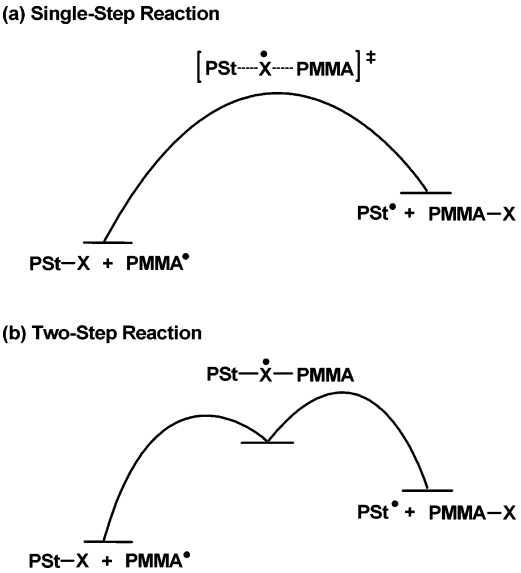

of $p_{deact} = 1$ ($C_{ex} \gg 110$), we have $p_{hh} = 0.025$, being more close to the literature value.

Block Copolymerizations of St and MMA. Besides the C_{ex} for the homopolymerizations of St and MMA, we determined the C_{ex} for their block copolymerizations, i.e., for PMMA−TeMe in the styrene polymerization and PSt−TeMe in the MMA polymerization, at 60 °C (Table 2). Interestingly, the C_{ex} values for PMMA• to PMMA−TeMe (homopolymerization) and PSt−TeMe (block copolymerization) were similar (17 vs 31), and those for PSt• to PSt−TeMe (homopolymerization) and PMMA−TeMe (block copolymerization) were also similar (3.6 vs 2.8). This means that the transfer of PSt block with MMA as well as that of PMMA block with St occurs efficiently to give the second PMMA or PSt block. These results are consistent with our previous observation of the controlled synthesis of diblock copolymers composed of St and MMA regardless of the order of monomer addition.[6,8,10]

Theoretical calculations suggest that the DT of organotellurium compounds proceeds through hypervalent tellurium intermediate or transition state (Scheme 3).[30,31] While the existence of trivalent tellurium radical intermediate has been still a controversial issue, the intermediate, if any, should locate very close in energy to the transition state. Therefore, the DT in TERP proceeds virtually through a single step without forming a kinetically important intermediate. The observed similarity in C_{ex} of the homo- and block copolymerizations must be attributed to similarity in the kinetic reactivity and/or the thermodynamic stability of PMMA• and PSt•. As a matter of fact, PSt• is known to be somewhat more reactive or less stable than PMMA•, which will explain the rather small differences among the observed C_{ex} values.

These results for TERP are in sharp contrast to those for RAFT polymerization which also proceeds via the DT mechanism. While C_{ex} values for PSt• to PSt-dithioacetate (−SCSMe) and PMMA−SCSMe were similar (220 vs 420), those for PMMA• to PMMA−SCSMe (homopolymerization) and PSt−SCSMe (block copolymerization) were very different (40 vs 0.83).[32,33] This kinetic result is consistent with the known fact that the block copolymerization of MMA to a PSt−SCSMe macroinitiator goes less successfully than that of St to the PMMA−SCSMe macroinitiator. The RAFT process proceeds through the well-defined intermediate, P−(SC•MeS)−P′,[34] the stability of which strongly depends on the polymer (alkyl) moieties P and P′. The intermediate with PMMA for both P and P′ is much less stable, or much faster to release P• or P′•, than the one with PSt for both P and P′. This difference in stability of the intermediates should be ascribed more to an entropic origin (e.g., the steric congestion around the P−S and P′−S bonds) rather than to an enthalpic one (e.g., the radical stability). In this regard, the PMMA−S bond with a tertiary carbon would be easier to be cleaved than the PSt−S bond with a secondary carbon, and thus the PMMA radical would be preferentially released from the hetero-intermediate PMMA−(SC•MeS)−PSt formed upon block copolymerization. This mechanistic difference in the DT (single-step vs two-step) for the two polymerizations explains why, in the block copolymer synthesis, the synthetic order (AB or BA block copolymerization) is less important for the TERP[6,8,10] than for the RAFT polymerization.[35]

Comparison of k_{ex}. Table 1 lists the k_p and k_{ex} at 60 °C. The k_p increases in the order of St (340 M^{-1} s^{-1})[22] < MMA (830)[23] ≪ VAc (9500)[36] < MA (24000),[13] and k_{ex} increases in the order of MMA (3000 M^{-1} s^{-1}) < St (5800) ≪ MA (4.6×10^5) < VAc (1.0×10^6 for the secondary adduct). In a rough generalization, systems small in k_p are also small in k_{ex}, and those large in k_p (MA and VAc) are also large in k_{ex}. The ratio k_{ex}/k_p (= C_{ex}) increased in the order of MMA (3.6) < St (17) ∼ MA (19) < VAc (110 for the secondary adduct) (Table 1).

In radical chemistry of small organic molecules, this type of chain transfer has been extensively studied as chalcogen group transfer for X = aryl chalcogens and halogen atom transfer for X = halogens.[37−41] The rate constants for phenyl-substituted chalcogen group transfer to a primary alkyl radical were generally similar to those for halogen atom transfer in the same row of the periodic table, if the displaced radical is the same.[37] For example, for the reaction with the octyl radical in benzene at 50 °C, $PhSeCH_2CO_2Et$ and $BrCH_2CO_2Et$ reacted with rate constants 1.0×10^5 and 0.7×10^5 M^{-1} s^{-1}, respectively, and $PhTeCH_2CO_2Et$ and ICH_2CO_2Et reacted with rate constants 2.3×10^7 and 2.6×10^7 M^{-1} s^{-1}, respectively.[37] The abstraction of Cl and SPh by tin radicals occurred at similar rates, and that of Br and SePh also occurred at similar rates.[38] These results suggested that phenyl-substituted chalcogen group transfer and halogen atom transfer are comparable in terms of the synthetic utility.[37] For the reaction with the phenyl vinyl radical (PhCH═CH•) in benzene at 80 °C, $PhTeCH(CH_3)_2$ reacted about 10 times faster than $ICH(CH_3)_2$.[39] Similar reactivity difference between TePh group and iodine has also been reported recently.[40] For the reaction with PSt• in styrene at 60 °C in our work, PSt−TeMe ($k_{ex} = 5700$ M^{-1} s^{-1}) reacted about 4 times faster than PSt-I (1400 M^{-1} s^{-1}) (Table 1). For these cases, tellurium group transfer is superior to iodine atom transfer in terms of the synthetic utility. The relative rates of the two transfers depend on the alkyl radical and the substituent on the chalcogen atom. Whereas further studies are needed to clarify the origin of reactivity differences between chalcogen groups and halogen atoms, these results strongly suggest that organo-chalcogen

compounds offer unique possibilities as the precursors of carbon-centered radicals over organo-halogen compounds in synthetic radical reactions.

Conclusions

The TERP of St, MMA, MA, and VAc was kinetically studied. For the homopolymerizations of St, MMA, and MA, the organotellurium had no detectable effect on R_p at examined temperatures (40−100 °C). For these systems, both thermal dissociation and degenerative chain transfer (DT) were involved in the activation process, and the main activation mechanism was DT at these temperatures. The C_{ex} largely depended on polymers (monomers) and increased in the order of MMA < St ∼ MA. The temperature dependences of C_{ex} for these systems were weak and negative. The VAc polymerization also included DT as the main activation process. The VAc polymerization suffers significant head-to-head addition on propagation, forming a primary alkyl chain-end (−CH_2−TeMe) adduct. The C_{ex} for this adduct was too small to achieve low polydispersity, explaining why the polydispersity control is not satisfactory at high degrees of polymerization of this monomer. The C_{ex} for PMMA$^{\bullet}$ to PMMA−TeMe (homopolymerization) and PSt−TeMe (block copolymerization) were similar, suggesting that the DT in TERP is a (nearly) single-step reaction without forming a kinetically important intermediate.

Acknowledgment. This work was supported by a Grant-in-Aid for Scientific Research, the Ministry of Education, Culture, Sports, Science and Technology, Japan (Grant-in-Aid 17002007).

Supporting Information Available: ^{1}H NMR spectrum of a poly(*n*-butyl acrylate) methyltelluride. This material is available free of charge via the Internet at http://pubs.acs.org.

References and Notes

(1) Matyjaszewski, K., Davis, T. P., Eds. *Handbook of Radical Polymerization*; Wiley-Interscience: New York, 2002.
(2) Matyjaszewski, K., Ed. *ACS Symp. Ser.* **1998**, *685*; **2000**, *768*; **2003**, *854*.
(3) (a) Matyjaszewski, K.; Xia, J. *Chem. Rev.* **2001**, *101*, 2921−2990. (b) Fischer, H. *Chem. Rev.* **2001**, *101*, 3581−3616. (c) Hawker, C. J.; Bosman, A. W.; Harth, E. *Chem. Rev.* **2001**, *101*, 3661−3688. (d) Kamigaito, M.; Ando, T.; Sawamoto, M. *Chem. Rev.* **2001**, *101*, 3689−3746. (e) Moad, G.; Rizzardo, E.; Thang, S. H. *Aust. J. Chem.* **2005**, *58*, 379−410.
(4) Fukuda, T. *J. Polym. Sci., Part A.: Polym. Chem.* **2004**, *42*, 4743−4755.
(5) Goto, A.; Fukuda, T. *Prog. Polym. Sci.* **2004**, *29*, 329−385.
(6) (a) Yamago, S. *Proc. Jpn. Acad., Ser. B* **2005**, *81*, 117−128. (b) Yamago, S. *J. Polym. Sci., Part A: Polym. Chem.* **2006**, *44*, 1−12.
(7) Yamago, S.; Iida, K.; Yoshida, J. *J. Am. Chem. Soc.* **2002**, *124*, 2874−2875.
(8) Yamago, S.; Iida, K.; Yoshida, J. *J. Am. Chem. Soc.* **2002**, *124*, 13666−13667.
(9) Yamago, S.; Iida, K.; Nakajima, M.; Yoshida, J. *Macromolecules* **2003**, *36*, 3793−3796.
(10) Yamago, S.; Iida, K.; Yoshida, J. *ACS Symp. Ser.* **2003**, *854*, 631−642.
(11) Goto, A.; Kwak, Y.; Fukuda, T.; Yamago, S.; Iida, K.; Nakajima, M.; Yoshida, J. *J. Am. Chem. Soc.* **2003**, *125*, 8720−8721.
(12) Grubisic, Z.; Rempp, P.; Benoit, H. *J. Polym. Sci., Part B: Polym. Lett.* **1967**, *5*, 753−759.
(13) Buback, M.; Kurz, C. H.; Schmaltz, C. *Macromol. Chem. Phys.* **1998**, *199*, 1721−1727.
(14) Atkinson, C. M. L.; Dietz, R. *Eur. Polym. J.* **1979**, *15*, 21−26.
(15) Goto, A.; Fukuda, T. *Macromolecules* **1997**, *30*, 5183−5186.
(16) Wakioka, M.; Baek, K. Y.; Ando, T.; Kamigaito, M.; Sawamoto, M. *Macromolecules* **2002**, *35*, 330−333.
(17) Goto, A.; Terauchi, T.; Fukuda, T.; Miyamoto, T. *Macromol. Rapid Commun.* **1997**, *18*, 673−681.
(18) Goto, A.; Ohno, K.; Fukuda, T. *Macromolecules* **1998**, *31*, 2809−2814.
(19) Fukuda, T.; Goto, A. *Macromol. Rapid Commun.* **1997**, *18*, 683−688: the factor −2 appearing in eq 4 is a misprint for $C - 2$.
(20) Kwak, Y.; Goto, A.; Fukuda, T.; Yamago, S.; Ray, B. *Z. Phys. Chem.* **2005**, *219*, 283−294.
(21) Goto, A.; Sato, K.; Tsujii, Y.; Fukuda, T.; Moad, G.; Rizzardo, E.; Thang, S. H. *Macromolecules* **2001**, *34*, 402−408.
(22) Gilbert, R. G. *Pure Appl. Chem.* **1996**, *68*, 1491−1494.
(23) Beuermann, S.; Buback, M.; Davis, T. P.; Gilbert, R. G.; Hutchinson, R. A.; Olaj, O. F.; Russell, G. T.; Schweer, J.; van Herk, A. M. *Macromol. Chem. Phys.* **1997**, *198*, 1545−1560.
(24) Asua, J. M.; Beuermann, S.; Buback, M.; Castignolles, P.; Charluex, B.; Gilbert, R. G.; Hutchinson, R. A.; Leiza, J. R.; Nikitin, A. N.; Vairon, J. P.; van Herk, A. M. *Macromol. Chem. Phys.* **2004**, *205*, 2151−2160.
(25) Willemse, R. X. E.; van Herk, A. M.; Panchenko, E.; Junkers, T.; Buback, M. *Macromolecules* **2005**, *38*, 5098−5103.
(26) Yamago, S.; Iida, K.; Yoshida, J., unpublished results.
(27) Iovu, M. C.; Matyjaszewski, K. *Macromolecules* **2003**, *36*, 9346−9354.
(28) Flory, P. J.; Leutner, F. S. *J. Polym. Sci.* **1948**, *3*, 880−890.
(29) Mayo, F. R. *J. Am. Chem. Soc.* **1943**, *65*, 2324−2329.
(30) Schiesser, C. H.; Smart, B. A. *Tetrahedron* **1995**, *51*, 6051−6060.
(31) Yamago, S.; Miyazoe, H.; Goto, R.; Hashidume, M.; Sawazaki, T.; Yoshida, J. *J. Am. Chem. Soc.* **2001**, *123*, 3697−3705.
(32) Fukuda, T.; Goto, A.; Kwak, Y.; Yoshikawa, C.; Ma, Y. D. *Macromol. Symp.* **2002**, *182*, 53−64.
(33) Kubo, K.; Goto, A.; Sato, K.; Kwak, Y.; Fukuda, T. *Polymer* **2005**, *46*, 9762−9768.
(34) Hawthorne, D. G.; Moad, G.; Rizzardo, E.; Thang, S. H. *Macromolecules* **1999**, *32*, 5457−5459.
(35) Chong, Y. K.; Le, T. P. T.; Moad, G.; Rizzardo, E.; Thang, S. H. *Macromolecules* **1999**, *32*, 2071−2074.
(36) Hutchinson, R. A.; Paquet, D. A., Jr.; McMinn, J. H.; Beuermann, S.; Fuller, R. E.; Jackson, C. *DECHEMA Monogr.* **1995**, *131*, 467−492.
(37) Curran, D. P.; Martin-Esker, A. A.; Ko, S.; Newcomb, M. *J. Org. Chem.* **1993**, *58*, 4691−4695.
(38) Beckwith, A. L. J.; Pigou, P. E. *Aust. J. Chem.* **1986**, *39*, 1151−1155.
(39) Han, L.; Ishihara, K.; Kambe, N.; Ogawa, A.; Ryu, I.; Sonoda, N. *J. Am. Chem. Soc.* **1992**, *114*, 7591−7592.
(40) (a) Kim, S.; Song, H.-J.; Choi, T.-L.; Yoon, J.-Y. *Angew. Chem., Int. Ed.* **2001**, *40*, 2524−2526. (b) Kim, S.; Song, H.-J. *Synlett* **2002**, 2110−2112.
(41) (a) Barton, D. H. R.; Ozbalik, N.; Sarma, J. C. *Tetrahedron Lett.* **1988**, *29*, 6581−6584. (b) Newcomb, M. *Tetrahedron* **1993**, *49*, 1151−1176. (c) Crich, D.; Chen, C.; Hwang, J.; Yuan, H.; Papadatos, A.; Walter, R. I. *J. Am. Chem. Soc.* **1994**, *116*, 8937−8951. (d) Schiesser, C. H.; Wild, L. M. *Tetrahedron* **1996**, *52*, 13265−13314. (e) Engman, L.; Gupta, V. *J. Org. Chem.* **1997**, *62*, 157−173. (f) Yamago, S. *Synlett* **2004**, 1875−1890.

MA060295M